Isotopologues Detection and Quantitative Analysis by Mid-infrared Dual-comb Laser Spectroscopy

Konstantin L. Vodopyanov

The College of Optics and Photonics (CREOL), University of Central Florida, Orlando, FL, USA

1	**Introduction**	1
2	**Frequency Combs and Their Spectroscopic Applications**	1
3	**Dual-comb Mid-IR System Based on Subharmonic Generation**	2
4	**Measurements with a Mixture of Gases**	4
5	**Molecular Detection in Ambient Air**	4
6	**Absolute Frequency Referencing and Resolution Limit**	5
7	**Detection Sensitivity**	6
8	**Future Dual-comb Systems for Ultrasensitive Isotopologues Detection**	8
9	**Conclusion and Outlook**	8
	Acknowledgments	8
	Abbreviations and Acronyms	8
	Related Articles	8
	References	8

Isotopologues are molecules that differ from the parent molecule only in their isotopic composition. For example, ordinary light water (H_2O), semi-heavy water (HDO), and heavy water (D_2O) are isotopologues of the same molecule. They have the same chemical formula and bonding arrangement of atoms, but at least one atom has a different number of neutrons than the parent. Isotopologues that differ only by the location of an isotopically modified element are called isotopomers. For example, the ^{15}N isotope in the N_2O molecule can be either next to the oxygen atom or second next to it; thus, $N^{15}NO$ and ^{15}NNO are isotopomers of the same molecule. Detecting isotopologues of different molecules is critical in such fields as astrobiology, biogeochemistry, personalized medicine, and forensics, with mass spectrometry being a major technique to distinguish between different isotopologues. In this article, I focus on a new technique for detection of isotopologues based on laser spectroscopy. The backbone of this technology is massively parallel spectroscopic probing in the mid-infrared spectral region by a frequency comb – a broad spectrum composed of some million phase-locked equidistant sharp spectral lines – produced by a subharmonic optical parametric oscillator (OPO). Through assessing their unique rotational-vibrational absorption signatures, we are able to simultaneously detect numerous molecules and their isotopologues in a mixture of gases, in real time and with one part-per-billion detection capability.

1 INTRODUCTION

Detecting isotopologues plays an important role in both scientific studies and applications. Numerous examples include chemistry,[1,2] biology and microbiology,[3,4] study of terrestrial biosphere,[5] geochemistry and geophysics,[6,7] astrophysics,[8,9] study of metabolic processes in biology and medicine,[10–12] medical diagnostic via breath analysis,[13,14] radiocarbon dating,[15,16] detecting the origins of prohibited drugs,[17] and in single-molecule surface-enhanced Raman spectroscopy.[18] Also, detection of isotopologues such as $^{13}C^{16}O$, HDO, and CH_3D in atmospheres of exoplanets (planets which orbit stars outside the solar system) through ground-based astronomical observations provide unique insights into planets' formation and evolution.[19]

Coherent laser beams provide unique prospect for sensing molecules through their resonant absorption features – either remotely or locally via multipass action. A privileged window for ultrasensitive molecular spectroscopy is the 3–20 μm portion of the mid-infrared (mid-IR) spectrum, where the strongest rotational-vibrational absorption lines can be addressed. For example, using mid-IR laser spectroscopy, the sensitivity of the measurement of radiocarbon dioxide ($^{14}CO_2$) with respect to the main isotopologue ($^{12}CO_2$), down to parts per quadrillion (10^{-15}) has already been demonstrated.[15] Thus, laser methods can successfully compete with mass spectrometry offering the benefits of compactness and much lower price. Figure 1 shows absorption lines of water molecule (H_2O) and its three isotopologues ($H_2{}^{18}O$, $H_2{}^{17}O$, and HDO). This example illustrates the richness of spectral information in the mid-IR region.

2 FREQUENCY COMBS AND THEIR SPECTROSCOPIC APPLICATIONS

Optical frequency combs – manifolds of evenly spaced and phase-locked narrow spectral lines produced by phase-stabilized femtosecond lasers – were introduced in the late 1990s and have revolutionized accurate measurements of frequency and time, as well as spectroscopic

Encyclopedia of Analytical Chemistry, Online © 2006–2020 John Wiley & Sons, Ltd.

This article was published in the *Encyclopedia of Analytical Chemistry* in 2020 by John Wiley & Sons, Ltd.
DOI: 10.1002/9780470027318.a9321

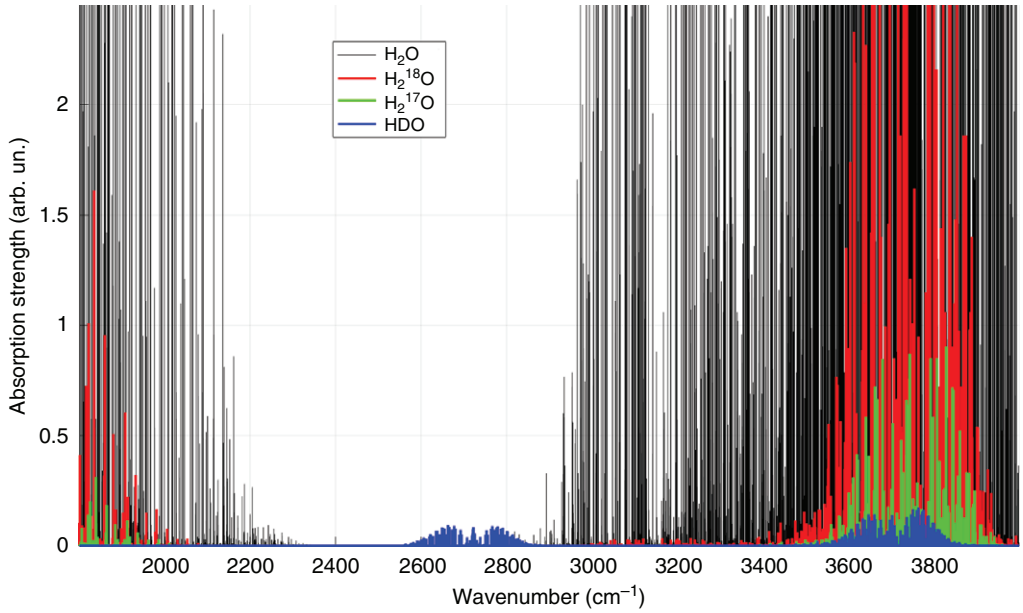

Figure 1 Infrared absorption spectra of the gas-phase water molecule (H_2O) and its three isotopologues ($H_2{}^{18}O$, $H_2{}^{17}O$, and HDO) in the mid-IR range of 1800–4000 cm^{-1} (wavelength range 2.5–5.5 μm). The plot was created using data from the HITRAN database. (Gordon et al.[20] Reproduced with permission of Elsevier.)

measurements,[21,22] and culminated in the 2005 Nobel Prize in Physics. Also, it has been shown that in spectroscopic applications, frequency combs can successfully compete with narrow-linewidth tunable lasers. Spectroscopic techniques with frequency combs include several scenarios: (i) where a broadband comb directly interrogates an absorbing sample after which the spectrum is dispersed in two dimensions and sensed with detector arrays,[23–25] (ii) a frequency comb is used as a light source in a Michelson-interferometer-based Fourier-transform spectroscopy,[26–30] and (iii) where two mutually coherent frequency-combs are superimposed and used to perform the dual-comb spectroscopy (DCS).[31–34] In the DCS method, a second frequency comb, with a small offset of mode spacing (same as an offset in the pulse repetition rate), effectively plays the role of the time-delayed second arm in the Michelson interferometer. However, this technique requires high degree of coherence between the two combs, and most reports that simultaneously take full advantage of the dual-comb technique (broad spectral coverage, comb-tooth resolved spectra, and rapid scans) have privileged, until recently, the near-infrared domain.[35–37]

Most recently, the advent of optical frequency combs in the 'signature' mid-IR region considerably improved both the precision and sensitivity of molecular detection.[38,39] Proof-of-principle demonstrations with frequency combs have been carried out by a number of groups in the wavelength region between 2.4 and 10 μm,[32,34,40–48] although with a limited instantaneous spectral coverage.

Ideally, for simultaneous detection of an assortment of molecules with different functional groups, one needs a spectrally broad frequency comb spanning an octave or more. Recently, it has been revealed that highly coherent and broad-bandwidth mid-IR combs can be created in a synchronously pumped OPO operating at *degeneracy*, which is also referred to as divide-by-2 subharmonic OPO or half-harmonic generator.[49–51] In such a divide-by-2 OPO, where the spectrum that spans well above an octave in the mid-IR can be produced, the output is inherently frequency- and phase-locked to the pump.[52] The *relative* linewidth between the comb teeth of the pump laser and its subharmonic has been measured to be well below 1 Hz.[53,54] This suggests high coherence of the generated OPO combs that allows long coherent averaging of the interferograms, which in its turn affects the signal-to-noise ratio of the acquired molecular spectrum.

3 DUAL-COMB MID-IR SYSTEM BASED ON SUBHARMONIC GENERATION

In our novel approach to DCS, we use a pair of highly coherent broadband subharmonic generators. The system starts with two optically referenced phase-locked thulium (Tm) fiber-laser frequency combs that pump two independent OPOs.[55] The lasers had the following

Encyclopedia of Analytical Chemistry, Online © 2006–2020 John Wiley & Sons, Ltd.

This article was published in the *Encyclopedia of Analytical Chemistry* in 2020 by John Wiley & Sons, Ltd.
DOI: 10.1002/9780470027318.a9321

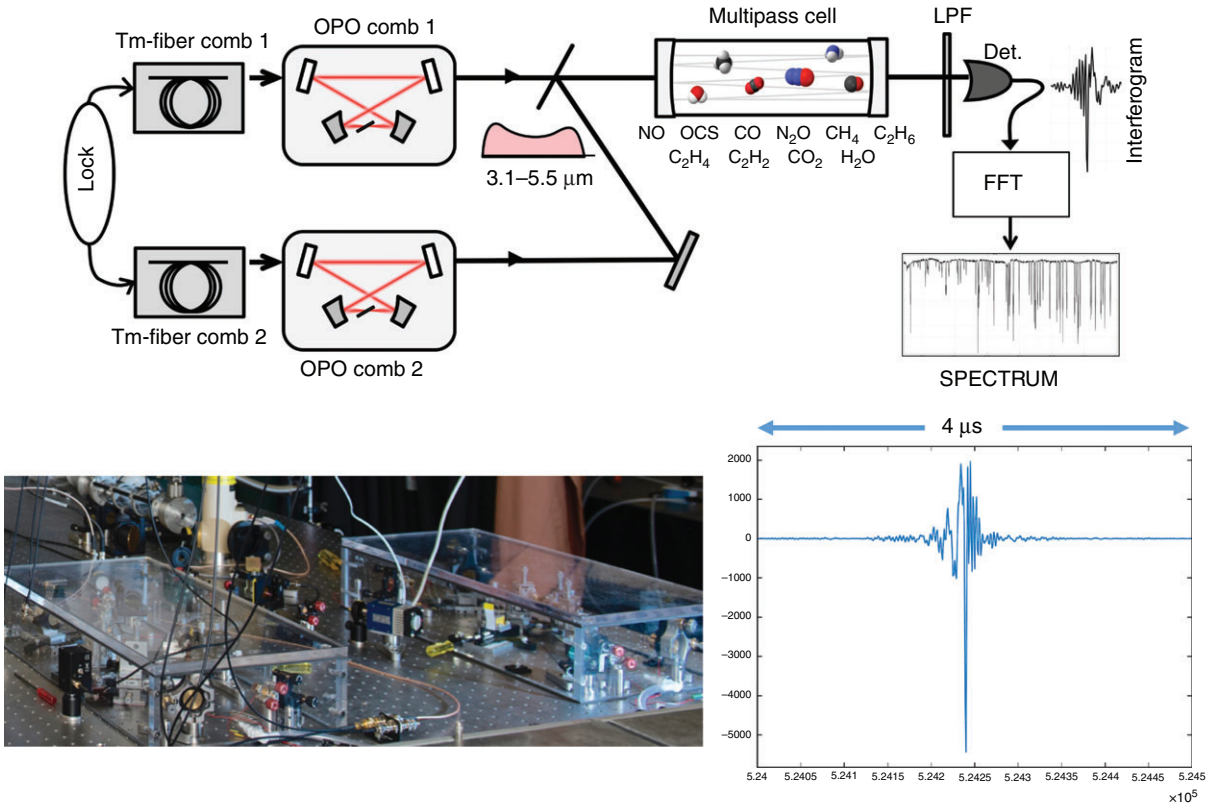

Figure 2 Schematic of the DCS setup. A pair of phase-locked Tm-fiber laser combs pumps a pair of subharmonic OPOs. Their beams are combined, passed through a 76-m multipass gas cell, detected with an InSb detector, digitized, and fast Fourier transformed to retrieve the optical spectrum. LPF, longpass (>2.5 μm) filter. The insets show the setup general view and the central portion of a typical interferogram.

parameters: central wavelength 1.93 μm, repetition rate f_{rep}=115 MHz, pulse duration 90 fs, and average power ~300 mW for each laser. To stabilize the frequency comb for each Tm laser, part of the oscillator light was amplified to generate a supercontinuum (SC) spanning 1–2.3 μm in a nonlinear silica fiber. While the 1.1- and 2.2-μm SC components were used to measure the carrier-envelope offset by *f*-to-2*f* interferometry,[53,56] the SC component near 1.56 μm was used get frequency beats with a stable continuous-wave (CW) reference diode laser. These two beat frequencies were coherently locked to fixed values, such that the frequency comb teeth had the same linewidth (3 kHz) as the CW reference.

The twin Tm-fiber comb system with an offset of repetition frequencies of $\Delta f_{rep} = 138.5$ Hz pumped two identical broadband subharmonic OPOs. Each OPO (Figure 2) had a ring-cavity bow-tie design with low roundtrip group delay dispersion achieved by using low-dispersion mirrors, a thin nonlinear gain crystal (0.5-mm-long orientation-patterned gallium arsenide, OP-GaAs) and a thin intracavity CaF_2 wedge (not shown in Figure 2) for the group-velocity dispersion control. The same wedge was used for the OPO beam outcoupling.[55] A low pump threshold of ~10 mW for each of the OPOs was typical for such a doubly resonant system.[52] The instantaneous spectral coverage of our DCS setup was 3.14–5.45 μm (1835–3185 cm^{-1}) at −25 dB level, set by the spectral overlap of the two OPOs.

The beams from the two OPOs with the average power of few mW in each beam were spatially combined, passed through a multi-pass gas cell (AMAC-76LW from Aerodyne, 76-m path length, 0.5-L volume) filled with a mixture of gases and sent to a detector (InSb from Kolmar, 77K, 60 MHz, long-wave cut-off 5.6 μm). The detector output was fed into a 16-bit analog-to-digital (AD) converter (AlazarTech, ATS9626). To avoid the folding of the dual-comb radiofrequency (RF) spectrum, the AD converter input was low-pass filtered to <50 MHz (for the bandwidth to be less than half of the frequency comb repetition rate).

The measurements were performed in the two regimes:

1. The comb-mode-resolved regime with a continuous recording of multiple interferograms over a time

Encyclopedia of Analytical Chemistry, Online © 2006–2020 John Wiley & Sons, Ltd.

This article was published in the *Encyclopedia of Analytical Chemistry* in 2020 by John Wiley & Sons, Ltd.
DOI: 10.1002/9780470027318.a9321

window of up to 40 s with no averaging. In this case, we were able to record the whole spectrum spanning 3.14–5.45 μm and resolve comb modes with a finesse of 4000.[55]

2. Recording single interferograms with the time window of $1/\Delta f_{rep} = 7.2$ ms, where up to more than 100 000 interferograms were coherently averaged in real time. In this regime, we acquired about 350 000 spectral data points spaced in frequency by the intermodal interval of 115 MHz. For the isotopologues study, this scenario was preferable since the measurements were much faster (from seconds to minutes) and required much less computer memory. The sampling interval of 115 MHz, corresponding to the mode spacing, was adequate for recording Doppler-broadened spectral features of the molecules under study. The inset to Figure 2 shows a typical DCS interferogram (its 4-μs portion of the full 7.2-ms record).

4 MEASUREMENTS WITH A MIXTURE OF GASES

To demonstrate parallel spectroscopic detection of multiple species, we filled the optical cell with a mixture of ten molecular gases: N_2O (nitrous oxide) at a concentration of 42 ppm, NO (nitric oxide) at 420 ppm, CO (carbon monoxide) at 120 ppm, OCS (carbonyl sulfide) at 26 ppm, CH_4 (methane) at 1500 ppm, C_2H_6 (ethane) at 490 ppm, C_2H_4 (ethylene) at 540 ppm, C_2H_2 (acetylene) at 6600 ppm, CO_2 (carbon dioxide) at 280 ppm, and H_2O (water vapor) at 2100 ppm. The buffer gas was N_2 and the total pressure 3 mbar. We coherently averaged single DCS interferograms, each with a time window of $1/\Delta f_{rep} = 7.2$ ms, with the total number of averages ranging from $N_{ave} = 100$ to 400 000.

A typical detector signal is shown in the inset to Figure 2 and the retrieved transmission optical spectra, after fast Fourier transforming the detector signal – in Figure 3. For a baseline (Figure 3a), we used the spectrum taken with the evacuated gas cell, where, atmospheric gases outside of the cell, mainly carbon dioxide and water vapor, contributed to the dips seen in this spectrum. The 'sample' spectrum (Figure 3b) – when the optical cell was filled with a mixture of gases – reveals characteristic absorption features of different molecules.

Figure 4 displays the absorbance spectra, $-\ln(T/T_0)$, where T is the transmission of the 'sample' cell and T_0 is that of the evacuated cell, for nine molecules – all that were used in the mixture of gases (except H_2O). Also shown are theoretical spectra (inverted in sign) from the high-resolution transmission molecular absorption (HITRAN) database for the given conditions. We

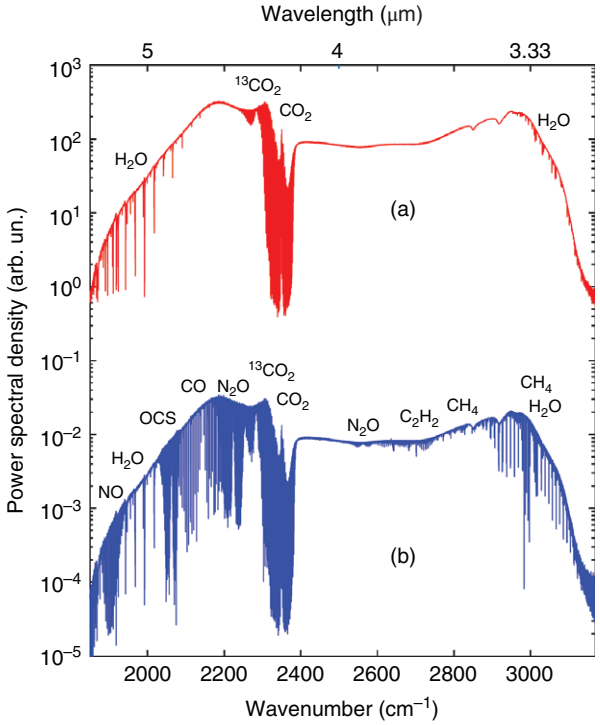

Figure 3 (a) Optical spectrum (log scale) retrieved from a single coherently averaged interferogram ($N_{ave} = 100\,000$) when the gas cell was evacuated. Absorption dips originate from atmospheric gases outside the cell. (b) Optical spectrum with the gas cell filled with a mixture of ten gases (OCS, N_2O, NO, CO, CH_4, C_2H_6, C_2H_4, C_2H_2, CO_2, and H_2O) in N_2 buffer gas at 3 mbar total pressure. The two curves are vertically offset for clarity.

observed an excellent matching to the HITRAN for all the molecules, in terms of peaks' center position and linewidth. In most cases, our spectral sampling (115 MHz or 0.004 cm^{-1}) was better than the Doppler broadened linewidths $\Delta\nu_D^{FWHM}$ of the molecules under study ($\Delta\nu_D^{FWHM}$ varied from 99 MHz for OCS to 283 MHz for CH_4).

With the above mixture of 10 molecules, we were able to detect and measure concentrations for 12 of their isotopologues that are present in small abundancies, 10^{-2}–10^{-4} with respect to the main molecule. These include $OC^{34}S$, $O^{13}CS$, $OC^{33}S$, $N^{15}NO$, ^{15}NNO, $N_2{}^{18}O$, ^{13}CO, $C^{18}O$, $^{13}CH_4$, $^{13}CO_2$, $C^{18}OO$, and $C^{17}OO$. Figure 5 shows the most prominent absorption peaks for these 12 isotopologues.

5 MOLECULAR DETECTION IN AMBIENT AIR

In a separate experiment, we measured DCS spectra of ambient air with the focus of detecting trace molecules and isotopologues. The gas cell was filled with room air

Encyclopedia of Analytical Chemistry, Online © 2006–2020 John Wiley & Sons, Ltd.

This article was published in the *Encyclopedia of Analytical Chemistry* in 2020 by John Wiley & Sons, Ltd.
DOI: 10.1002/9780470027318.a9321

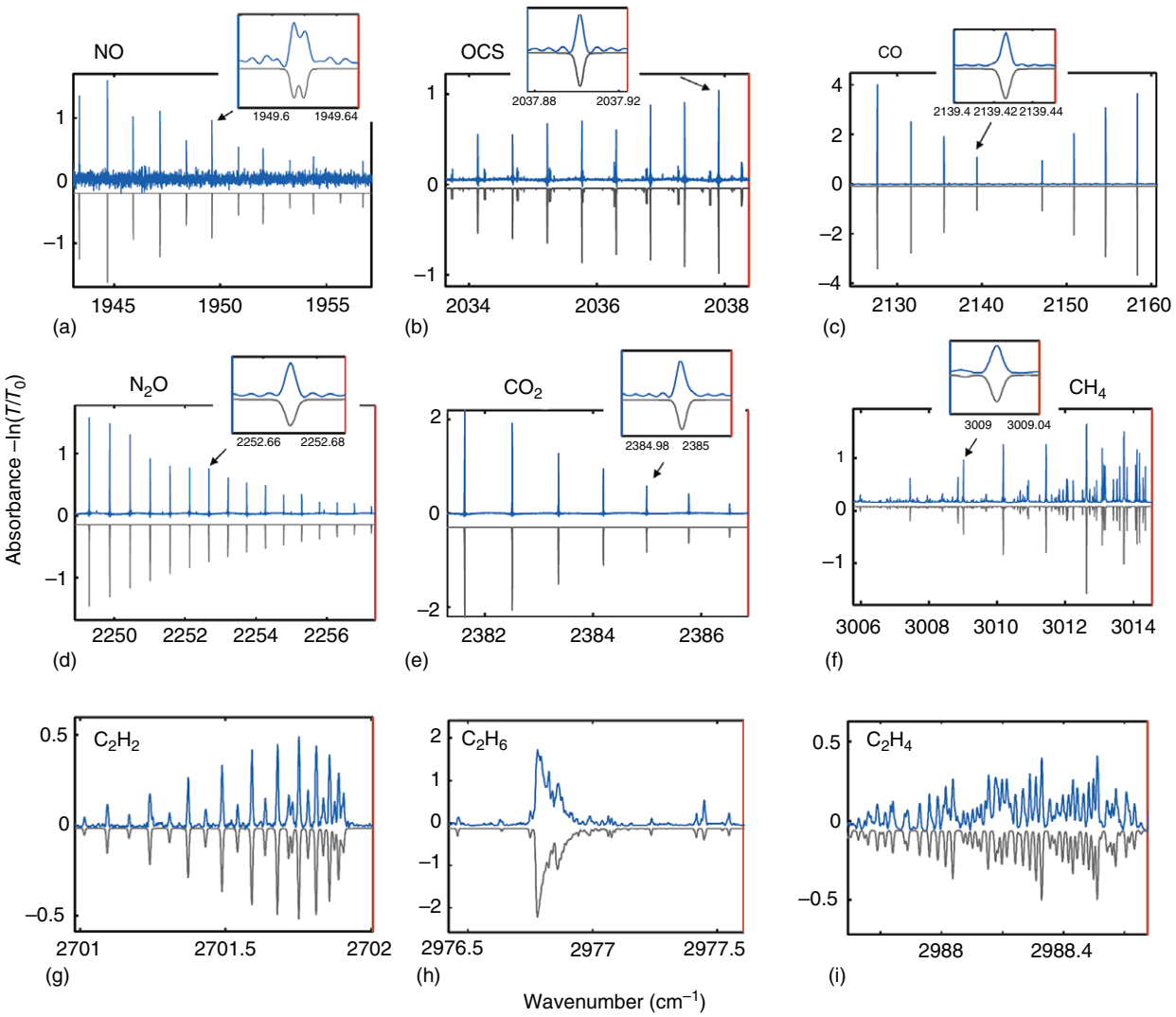

Figure 4 Absorbance spectra for nine molecules (N_2 buffer gas with 3-mbar total pressure) obtained by normalizing the 'sample' spectrum to that of the empty-cell spectrum of Figure 3. Also shown are theoretical (HITRAN database) absorption spectra, which are inverted for clarity (theoretical peaks are looking down).

at $p = 10$ mbar and single interferograms were coherently averaged. In addition to water and CO_2, we detected and quantified nine other molecules naturally present in the atmosphere in trace amounts, with their spectra shown in Figure 6. These molecules are CO at a concentration of 280 ppb (parts-per-billion), N_2O at 240 ppb, CH_4 at 1.4 ppm, three isotopologues of CO_2:$^{13}CO_2$, $C^{18}OO$, and $C^{17}OO$ at 3 ppm, 1.3 ppm, and 220 ppb respectively, and three isotopologues of water: $H_2{}^{18}O$, $H_2{}^{17}O$, and HDO at 160, 30, and 25 ppm, respectively. With $N_{ave} = 100\,000$ (12 min recording time) the characteristic peaks of HDO were detected with a signal-to-noise ratio of ~100. For each of the above molecules in air, the concentration was derived via comparison of absorption peaks' strength with the HITRAN simulations.

6 ABSOLUTE FREQUENCY REFERENCING AND RESOLUTION LIMIT

Our optical spectra were referenced to radio frequencies only: the frequency counters for measuring f_{rep} and Δf_{rep}, the frequency synthesizers that generated offsets for Tm-fiber combs, and the clock of the A/D card – were all stabilized against a 10 MHz quartz oscillator locked to a Rb-clock (FS725 from Stanford Research Systems). Its absolute accuracy of $\sim 10^{-10}$ corresponds to ~8 kHz accuracy of the absolute optical referencing.

In principle, one can achieve the spectral resolution on the order of the absolute comb linewidth (3 kHz)

Encyclopedia of Analytical Chemistry, Online © 2006–2020 John Wiley & Sons, Ltd.

This article was published in the *Encyclopedia of Analytical Chemistry* in 2020 by John Wiley & Sons, Ltd.
DOI: 10.1002/9780470027318.a9321

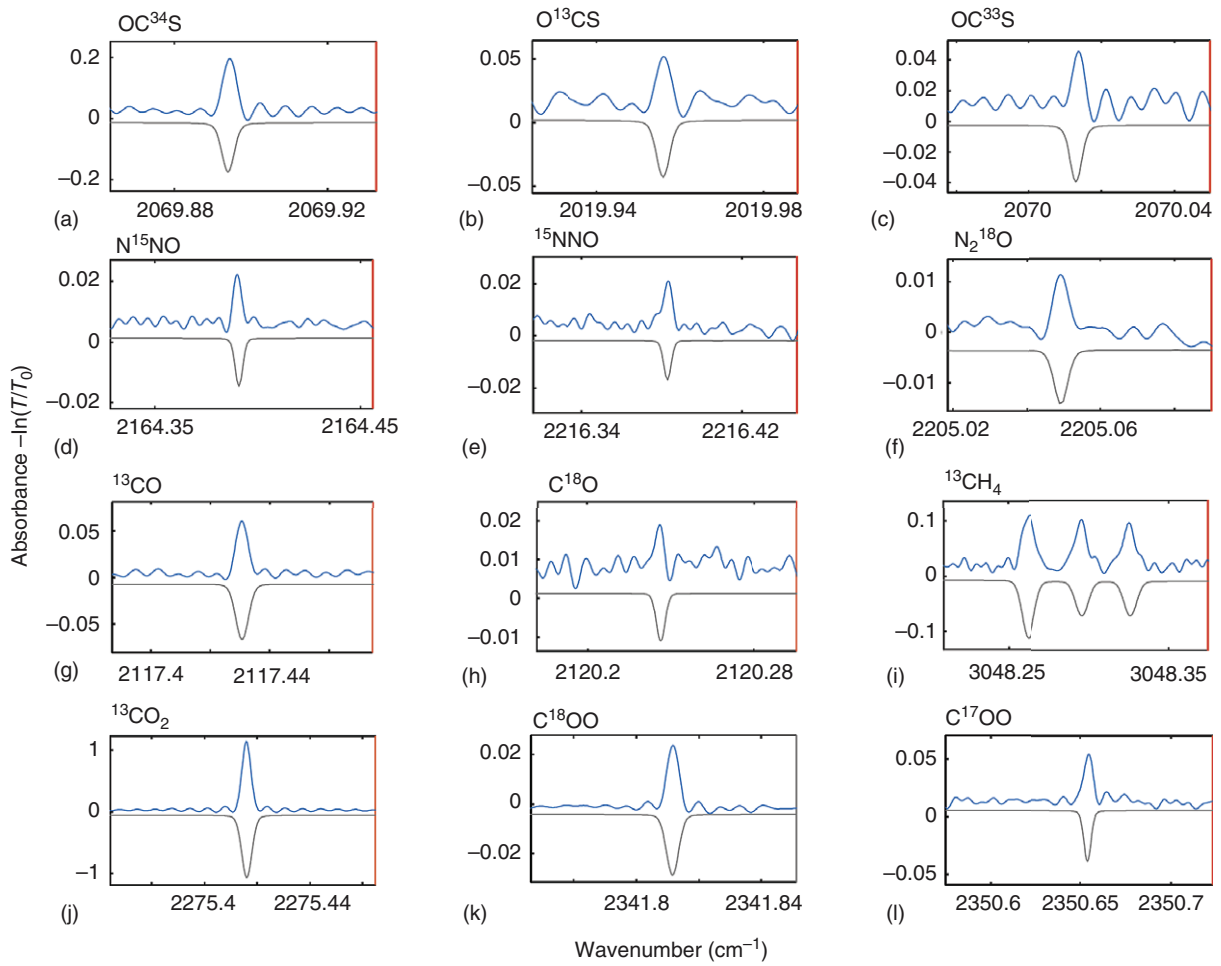

Figure 5 Spectra of isotopologues detected in a mixture of gases at 3 mbar. (a) $OC^{34}S$, (b) $O^{13}CS$, (c) $OC^{33}S$, (d) $N^{15}NO$, (e) ^{15}NNO, (f) $N_2{}^{18}O$, (g) ^{13}CO, (h) $C^{18}O$, (i) $^{13}CH_4$, (j) $^{13}CO_2$, (k) $C^{18}OO$, (l) $C^{17}OO$. Also shown are theoretical (HITRAN) absorption spectra, which are inverted for clarity.

by taking comb-tooth resolved spectra and repeating measurements with frequency-shifted combs (so-called interleaving of the comb spectra).

7 DETECTION SENSITIVITY

Table 1 displays minimal detectable concentrations for different molecules and their isotopologues obtained in our experiment with a setup that uses a multipass cell with the path distance of 76 m, and the acquisition time of 720 s. (For shorter acquisition times τ, the signal-to-noise ratio scales as $\sqrt{\tau}$.) Here, we define the minimal detectable concentration is such a way that the corresponding absorbance is 3σ, where σ is the laser noise – relative standard deviation of the spectral power density in a given spectral region. For example, at $\tau = 720$ s ($N_{ave} = 100\,000$), in the central part of our detection band $\sigma \approx 10^{-3}$, which means that we can detect absorption peaks that are 0.3% deep.

The above detection limits can be further improved by using the following two strategies:

1. One strength of DCS is that it uses only a single detector to record millions of spectral points. However, the downside is the so-called 'multiplexed penalty' – the spectral noise increases as the number of spectral elements (comb teeth) M increases. As a result, the signal-to-noise ratio in DCS scales as $\sqrt{\tau}/M$.[33] Consequently, reducing the bandwidth of the frequency comb and limiting it to the range of the strongest absorption features for the molecules of interest can improve SNR in the dual-comb measurements. This can be done either by using an optical filter or, in some occasions, by adjustment of the OPO cavity parameters. Unless

Encyclopedia of Analytical Chemistry, Online © 2006–2020 John Wiley & Sons, Ltd.

This article was published in the *Encyclopedia of Analytical Chemistry* in 2020 by John Wiley & Sons, Ltd.
DOI: 10.1002/9780470027318.a9321

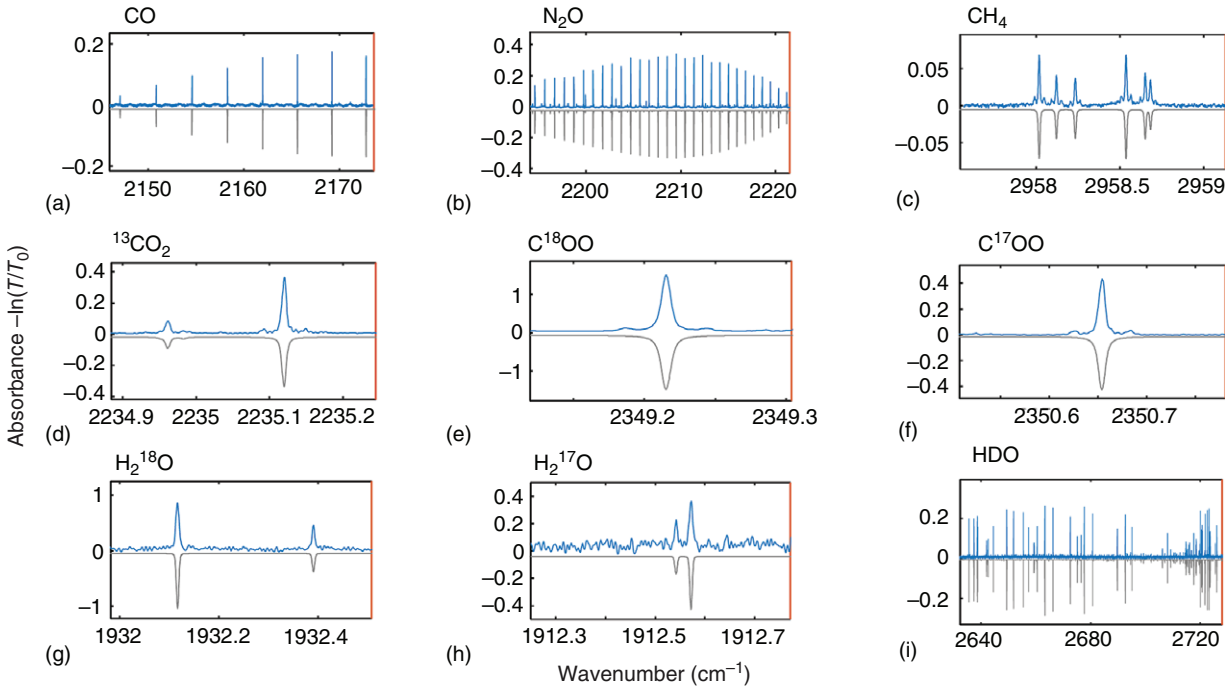

Figure 6 Spectra of trace molecules in ambient air taken at 10-mbar pressure. (a) CO, (b) N_2O, (c) CH_4, (d–f) three isotopologues of CO_2, (g–i) three isotopologues of water. Also shown are theoretical (HITRAN) absorption spectra, which are inverted for clarity.

Table 1 Detection limits for different molecules (and their isotopologues)

Molecule (including isotopologues)	Detection limit (3σ) with the acquisition time of 720 s and full bandwidth 3.1–5.5 μm (1350 cm^{-1})	Detection limit (3σ) with the acquisition time of 720 s, reduced bandwidth (100–150 cm^{-1}), and multi-line analysis
CO_2	2 ppb	30 ppt
CO	11 ppb	160 ppt
CH_4	105 ppb	1.5 ppb
OCS	9 ppb	130 ppt
N_2O	7 ppb	100 ppt
HDO	90 ppb	1.3 ppb

one needs massive parallelism of molecular detection, one can reduce the spectral band from, e.g. 1350 cm^{-1} to 100–150 cm^{-1}, which is a typical value for ro-vibrational bands.

2. An important advantage of broadband spectroscopy, such as DCS, is the ability to detect multiple absorption peaks. This allows achieving lower detectable concentrations than with single-peak measurements. When applied to broadband spectra, the multi-line analysis can significantly (by $\sim\sqrt{N}$, where N is the number of peaks) decrease the concentration detection limits.[19,27,57,58] Typically, such methods as cross-correlation are used for spectrum characterization, where the theoretical noise-free spectrum from a database is used as a cross-correlation template. Overall, multi-line analysis can improve the sensitivity by a factor of 5–10. For example, by applying cross-correlation with the HITRAN spectrum, we were able to identify the $C^{17}O$ isotopologue in a mixture of gases, as of Figure 5, despite the fact that the natural abundance of $C^{17}O$ (3.7×10^{-4} with respect to the parent CO molecule) is very low, 5.5 times smaller than that of $C^{18}O$, whose absorption peaks were barely detectable in the DCS spectrum. Shown in the last column of Table 1 are minimal detectable concentrations that can be achieved when the two above approaches for sensitivity enhancement are used.

Encyclopedia of Analytical Chemistry, Online © 2006–2020 John Wiley & Sons, Ltd.

This article was published in the *Encyclopedia of Analytical Chemistry* in 2020 by John Wiley & Sons, Ltd.
DOI: 10.1002/9780470027318.a9321

Finally, it is worth noticing that the optical absorption spectroscopy provides the capability of absolute isotopologues' concentration measurements. This is based on the fact that once the optical absorbance is measured in experiment, one can easily extract the absolute concentration for a given type of molecule using known absorption cross-sections (from existing databases), optical path length, and the total pressure of the gas.

8 FUTURE DUAL-COMB SYSTEMS FOR ULTRASENSITIVE ISOTOPOLOGUES DETECTION

To realize the full potential of the DCS approach, new systems are under study in our group, that would allow extending the combs into the long wave-infrared and THz regions. One particular project involves a subharmonic OPO setup that uses a newly developed nonlinear-optical crystal, orientation-patterned gallium phosphide (OP-GaP), pumped by an ultrafast 2.35-μm Cr:ZnS solid state laser. The OPO produces a record-wide instantaneous output spectrum of 3–12.5 μm that is more than two octaves in frequency span.[59] The next step for this development is building a pair of phase-locked OPOs to be used in spectroscopic detection with dual frequency combs.

9 CONCLUSION AND OUTLOOK

Based on the strongest molecular tell-tale vibrational bands, we demonstrated parallel detection and quantification of numerous molecular species in a mixture, including isotopologues containing ^{13}C, ^{18}O, ^{17}O, ^{15}N, ^{34}S, ^{33}S, and ^{2}H (deuterium), with ppb-level sensitivity, which can be improved to part-per-trillion level. We believe our demonstration reveals all the benefits of DCS technique in the mid-IR, including rapid scans (seconds to minutes), broad spectral coverage, high (sub-Doppler) spectral resolution, absolute optical frequency referencing, superior detection sensitivity, discrimination against other absorbing species, and capability of absolute concentration measurements with no need for prior calibration.

ACKNOWLEDGMENTS

This work has been supported by the Office of Naval Research (ONR) (N00014-15-1-2659) and Defense Advanced Research Projects Agency (DARPA) (W31P4Q-15-1-0008) grants. The author would also like to thank the researchers and students in his group who participated in this project.

ABBREVIATIONS AND ACRONYMS

AD	Analog-to-digital
CW	Continuous-wave
DCS	Dual-comb Spectroscopy
HDO	Semi-heavy Water
HITRAN	High-resolution Transmission Molecular Absorption
mid-IR	Mid-infrared
OP-GaP	Orientation-patterned Gallium Phosphide
OPO	Optical Parametric Oscillator
ppb	Parts-per-billion
RF	Radiofrequency
SC	Supercontinuum

RELATED ARTICLES

Environment: Trace Gas Monitoring
Precision Molecular Spectroscopy with Frequency Combs

REFERENCES

1. H.C. Urey, 'The Thermodynamic Properties of Isotopic Substances', *J. Chem. Soc. London*, 562–581 (1947).
2. M. Turowski, N. Yamakawa, J. Meller, K. Kimata, T. Ikegami, K. Hosoya, N. Tanaka, E.R. Thornton, 'Deuterium Isotope Effects on Hydrophobic Interactions: The Importance of Dispersion Interactions in the Hydrophobic Phase', *J. Am. Chem. Soc.*, **125**, 13836–13849 (2003).
3. M. Cuntz, J. Ogee, G.D. Farquhar, P. Peylin, L.A. Cernusak, 'Modelling Advection and Diffusion of Water Isotopologues in Leaves', *Plant Cell Environ.*, **30**, 892–909 (2007).
4. H.W. Hu, D. Chen, J.Z. He, 'Microbial Regulation of Terrestrial Nitrous Oxide Formation: Understanding the Biological Pathways for Prediction of Emission Rates', *FEMS Microbiol. Rev.*, **39**, 729–749 (2015).
5. J.M. Eiler, E. Schauble, '(OCO)-O-18-C-13-O-16 in Earth's Atmosphere', *Geochim. Cosmochim. Acta*, **68**, 4767–4777 (2004).
6. P. Ghosh, J. Adkins, H. Affek, B. Balta, W. Guo, E.A. Schauble, D. Schrag, J.M. Eiler, '^{13}C–^{18}O Bonds in Carbonate Minerals: A New Kind of Paleothermometer', *Geochim. Cosmochim. Acta*, **70**, 1439–1456 (2006).

This article was published in the *Encyclopedia of Analytical Chemistry* in 2020 by John Wiley & Sons, Ltd.
DOI: 10.1002/9780470027318.a9321

7. H.P. Affek, J.M. Eiler, 'Abundance of Mass 47 CO_2 in Urban Air, Car Exhaust, and Human Breath', *Geochim. Cosmochim. Acta*, **70**, 1–12 (2006).
8. V. Pietu, A. Dutrey, S. Guilloteau, 'Probing the Structure of Protoplanetary Disks: A Comparative Study of DM Tau, LkCa 15, and MWC 480', *Astron. Astrophys.*, **467**, 163–178 (2007).
9. B. Parise, C. Ceccarelli, A.G.G.M. Tielens, A. Castets, E. Caux, B. Lefloch, S. Maret, 'Testing Grain Surface Chemistry: A Survey of Deuterated Formaldehyde and Methanol in Low-Mass Class 0 Protostars', *Astron. Astrophys.*, **453**, 949–958 (2006).
10. W.H.W. Tang, Z.E. Wang, B.S. Levison, R.A. Koeth, E.B. Britt, X.M. Fu, Y.P. Wu, S.L. Hazen, 'Intestinal Microbial Metabolism of Phosphatidylcholine and Cardiovascular Risk', *N. Engl. J. Med.*, **368**, 1575–1584 (2013).
11. W. Eisenreich, T. Dandekar, J. Heesemann, W. Goebel, 'Carbon Metabolism of Intracellular Bacterial Pathogens and Possible Links to Virulence', *Nat. Rev. Microbiol.*, **8**, 401–412 (2010).
12. S. Marsch, A. Bacher, C. Ettenhuber, T. Grawert, H. Muckter, D. Seidel, M. Vogeser, R. Laupitz, M. Fischer, U. Bacher, W. Eisenreich, 'The Complex Isotopologue Space of Glucose as a Framework for the Study of Human Intermediary Metabolism', *Isot. Environ. Health Stud.*, **51**, 11–23 (2015).
13. E.R. Crosson, K.N. Ricci, B.A. Richman, F.C. Chilese, T.G. Owano, R.A. Provencal, M.W. Todd, J. Glasser, A.A. Kachanov, B.A. Paldus, T.G. Spence, R.N. Zare, 'Stable Isotope Ratios Using Cavity Ring-down Spectroscopy: Determination of C-13/C-12 for Carbon Dioxide in Human Breath', *Anal. Chem.*, **74**, 2003–2007 (2002).
14. T.S. Chen, F.Y. Chang, P.C. Chen, T.W. Huang, J.T. Ou, M.H. Tsai, M.S. Wu, J.T. Lin, 'Simplified 13C-urea Breath Test with a New Infrared Spectrometer for Diagnosis of *Helicobacter pylori* Infection', *J. Gastroenterol. Hepatol.*, **18**, 1237–1243 (2003).
15. I. Galli, S. Bartalini, R. Ballerini, M. Barucci, P. Cancio, M. De Pas, G. Giusfredi, D. Mazzotti, N. Akikusa, P. De Natale, 'Spectroscopic Detection of Radiocarbon Dioxide at Parts-per-quadrillion Sensitivity', *Optica*, **3**, 385–388 (2016).
16. J. Karhu, T. Tomberg, F.S. Vieira, G. Genoud, V. Hänninen, M. Vainio, M. Metsälä, T. Hieta, S. Bell, L. Halonen, 'Broadband Photoacoustic Spectroscopy of $^{14}CH_4$ with a High-power Mid-infrared Optical Frequency Comb', *Opt. Lett.*, **44**, 1142–1145 (2019).
17. G. Ambrosio, X. de la Torre, M. Mazzarino, M.K. Parr, F. Botre, 'Effect of Non-prohibited Drugs on the Phase II Metabolic Profile of Morphine. An In Vitro Investigation for Doping Control Purposes', *Drug Test. Anal.*, **10**, 984–994 (2018).
18. J.A. Dieringer, R.B. Lettan, K.A. Scheidt, R.P. Van Duyne, 'A Frequency Domain Existence Proof of Single-molecule Surface-enhanced Raman Spectroscopy', *J. Am. Chem. Soc.*, **129**, 16249–16256 (2007).
19. P. Mollière, I. A. G. Snellen, 'Detecting Isotopologues in Exoplanet Atmospheres Using Ground-Based High-dispersion Spectroscopy', *arXiv:1809.01156v2* (2019).
20. I. Gordon, L. Rothman, C. Hill, R. Kochanov, Y. Tan, P. Bernath, M. Birk, V. Boudon, A. Campargue, K. Chance, B. Drouin, J.-M. Flaud, R. Gamache, J. Hodges, D. Jacquemart, V. Perevalov, A. Perrin, K. Shine, M.-A. Smith, J. Tennyson, G. Toon, H. Tran, V. Tyuterev, A. Barbe, A. Csszr, V. Devi, T. Furtenbacher, J. Harrison, J.-M. Hartmann, A. Jolly, T. Johnson, T. Karman, I. Kleiner, A. Kyuberis, J. Loos, O. Lyulin, S. Massie, S. Mikhailenko, N. Moazzen-Ahmadi, H. Mller, O. Naumenko, A. Nikitin, O. Polyansky, M. Rey, M. Rotger, S. Sharpe, K. Sung, E. Starikova, S. Tashkun, J.V. Auwera, G. Wagner, J. Wilzewski, P. Wciso, S. Yu, E. Zak, 'The HITRAN2016 Molecular Spectroscopic Database', *J. Quant. Spectrosc. Radiat. Transf.*, **203**, 3–69 (2017).
21. T. Udem, R. Holzwarth, T.W. Hänsch, 'Optical Frequency Metrology', *Nature*, **416**, 233–237 (2002).
22. D. Gatti, T. Sala, M. Marangoni, G. Galzerano, L. Gianfrani, 'Precision Molecular Spectroscopy with Frequency Combs', in *Encyclopedia of Analytical Chemistry: Applications, Theory and Instrumentation*, Wiley, 2011. DOI: 10.1002/9780470027318.a9249
23. S.A. Diddams, L. Hollberg, V. Mbele, 'Molecular Fingerprinting with the Resolved Modes of a Femtosecond Laser Frequency Comb', *Nature*, **445**, 627–630 (2007).
24. L. Nugent-Glandorf, T. Neely, F. Adler, A.J. Fleisher, K.C. Cossel, B. Bjork, T. Dinneen, J. Ye, S.A. Diddams, 'Mid-infrared Virtually Imaged Phased Array Spectrometer for Rapid and Broadband Trace Gas Detection', *Opt. Lett.*, **37**, 3285–3287 (2012).
25. A.J. Fleisher, B.J. Bjork, T.Q. Bui, K.C. Cossel, M. Okumura, J. Ye, 'Mid-infrared Time-resolved Frequency Comb Spectroscopy of Transient Free Radicals', *J. Phys. Chem. Lett.*, **5**, 2241–2246 (2015).
26. A. Foltynowicz, P. Maslowski, T. Ban, F. Adler, K.C. Cossel, T.C. Briles, J. Ye, 'Optical Frequency Comb Spectroscopy', *Faraday Discuss.*, **150**, 23–31 (2011).
27. M.W. Haakestad, T.P. Lamour, N. Leindecker, A. Marandi, K.L. Vodopyanov, 'Intracavity Trace Molecular Detection with a Broadband Mid-IR Frequency Comb Source', *J. Opt. Soc. Am. B*, **30**, 631–640 (2013).
28. S.A. Meek, A. Poisson, G. Guelachvili, T.W. Hänsch, N. Picqué, 'Fourier Transform Spectroscopy Around 3 μm with a Broad Difference Frequency Comb', *Appl. Phys. B Lasers Opt.*, **114**(4), 573–578 (2014).
29. A. Khodabakhsh, V. Ramaiah-Badarla, L. Rutkowski, A.C. Johansson, K.F. Lee, J. Jiang, C. Mohr, M.E.

Encyclopedia of Analytical Chemistry, Online © 2006–2020 John Wiley & Sons, Ltd.

This article was published in the *Encyclopedia of Analytical Chemistry* in 2020 by John Wiley & Sons, Ltd.
DOI: 10.1002/9780470027318.a9321

Fermann, A. Foltynowicz, 'Fourier Transform and Vernier Spectroscopy Using an Optical Frequency Comb at 3–5.4 μm', *Opt. Lett.*, **41**, 2541–2544 (2016).

30. P. Maslowski, K.F. Lee, A.C. Johansson, A. Khodabakhsh, G. Kowzan, L. Rutkowski, A.A. Mills, C. Mohr, J. Jiang, M.E. Fermann, A. Foltynowicz, 'Surpassing the Path-limited Resolution of Fourier-transform Spectrometry with Frequency Combs', *Phys. Rev. A*, **93**(R), 021802 (2016).
31. F. Keilmann, C. Gohle, R. Holzwarth, 'Time-domain Mid-infrared Frequency-comb Spectrometer', *Opt. Lett.*, **29**, 1542–1544 (2004).
32. A. Schliesser, M. Brehm, F. Keilmann, D.W. van der Weide, 'Frequency-comb Infrared Spectrometer for Rapid, Remote Chemical Sensing', *Opt. Express*, **13**, 9029–9038 (2005).
33. I. Coddington, N. Newbury, W. Swann, 'Dual-comb Spectroscopy', *Optica*, **3**, 414–426 (2016).
34. G. Villares, A. Hugi, S. Blaser, J. Faist, 'Dual-comb Spectroscopy Based on Quantum-cascade-laser Frequency Combs', *Nat. Commun.*, **5**, 5192 (2014).
35. I. Coddington, W.C. Swann, N.R. Newbury, 'Coherent Multiheterodyne Spectroscopy Using Stabilized Optical Frequency Combs', *Phys. Rev. Lett.*, **100**, 013902 (2008).
36. I. Coddington, W.C. Swann, N.R. Newbury, 'Time-domain Spectroscopy of Molecular Free-induction Decay in the Infrared', *Opt. Lett.*, **35**, 1395–1397 (2010).
37. M. Zolot, F.R. Giorgetta, E. Baumann, J.W. Nicholson, W.C. Swann, I. Coddington, N.R. Newbury, 'Direct-comb Molecular Spectroscopy with Accurate, Resolved Comb Teeth Over 43 THz', *Opt. Lett.*, **37**, 638–640 (2012).
38. A. Schliesser, N. Picqué, T.W. Hänsch, 'Mid-infrared Frequency Combs', *Nat. Photonics*, **6**, 440–449 (2012).
39. N. Picqué, T.W. Hänsch, 'Frequency Comb Spectroscopy', *Nat. Photonics*, **13**, 146–157 (2019).
40. B. Bernhardt, E. Sorokin, P. Jacquet, R. Thon, T. Becker, I.T. Sorokina, N. Picqué, T.W. Hänsch, 'Mid-infrared Dual-comb Spectroscopy with 2.4 μm Cr^{2+}:ZnSe Femtosecond Lasers', *Appl. Phys. B Lasers Opt.*, **100**, 3–8 (2010).
41. Z. Zhang, T. Gardiner, D.T. Reid, 'Mid-infrared Dual-comb Spectroscopy with an Optical Parametric Oscillator', *Opt. Lett.*, **38**, 3148–3150 (2013).
42. F.C. Cruz, D.L. Maser, T. Johnson, G. Ycas, A. Klose, F.R. Giorgetta, I. Coddington, S.A. Diddams, 'Mid-infrared Optical Frequency Combs Based on Difference Frequency Generation for Molecular Spectroscopy', *Opt. Express*, **23**, 26814–26824 (2015).
43. Y.W. Jin, S.M. Cristescu, F.J.M. Harren, J. Mandon, 'Femtosecond Optical Parametric Oscillators Toward Real-time Dual-comb Spectroscopy', *Appl. Phys. B Lasers Opt.*, **119**, 65–74 (2015).
44. F. Zhu, A. Bicer, R. Askar, J. Bounds, A. Kolomenskii, V. Kelessides, M. Amani, H. Schuessler, 'Mid-infrared Dual Frequency Comb Spectroscopy Based on Fiber Lasers for the Detection of Methane in Ambient Air', *Laser Phys. Lett.*, **12**, 095701 (2015).
45. O. Kara, Z. Zhang, T. Gardiner, D.T. Reid, 'Dual-comb Mid-infrared Spectroscopy with Free-running Oscillators and Absolute Optical Calibration from a Radio-Frequency Reference', *Opt. Express*, **25**, 16072–16082 (2017).
46. L. Maser, G. Ycas, W.I. Depetri, F.C. Cruz, S.A. Diddams, 'Coherent Frequency Combs for Spectroscopy Across the 3–5 μm Region', *Appl. Phys. B Lasers Opt.*, **123**, 142 (2017).
47. E. Baumann, F.R. Giorgetta, W.C. Swann, A.M. Zolot, I. Coddington, N.R. Newbury, 'Spectroscopy of the Methane $\nu 3$ Band with an Accurate Midinfrared Coherent Dual-comb Spectrometer', *Phys. Rev. A*, **84**, 062513 (2011).
48. G. Ycas, F.R. Giorgetta, E. Baumann, I. Coddington, D. Herman, S.A. Diddams, N.R. Newbury, 'High-coherence Mid-infrared Dual-comb Spectroscopy Spanning 2.6 to 5.2 μm', *Nat. Photonics*, **12**, 202–208 (2018).
49. K.L. Vodopyanov, S.T. Wong, and R.L. Byer, 'Infrared Frequency Comb Methods, Arrangements and Applications', U.S. patent 8,384,990 (February 26, 2013).
50. N. Leindecker, A. Marandi, R.L. Byer, K.L. Vodopyanov, 'Broadband Degenerate OPO for Mid-infrared Frequency Comb Generation', *Opt. Express*, **19**(6304–6310) (2011).
51. A. Marandi, N.C. Leindecker, V. Pervak, R.L. Byer, K.L. Vodopyanov, 'Coherence Properties of a Broadband Femtosecond Mid-IR Optical Parametric Oscillator Operating at Degeneracy', *Opt. Express*, **20**, 7255–7262 (2012).
52. V.O. Smolski, H. Yang, S.D. Gorelov, P.G. Schunemann, K.L. Vodopyanov, 'Coherence Properties of a 2.6-7.5-μm Frequency Comb Produced as Subharmonic of a Tm-fiber Laser', *Opt. Lett.*, **41**, 1388–1391 (2016).
53. K.F. Lee, N. Granzow, M.A. Schmidt, W. Chang, L. Wang, Q. Coulombier, J. Troles, N. Leindecker, K.L. Vodopyanov, P.G. Schunemann, M.E. Fermann, P.St.J. Russell, I. Hartl, 'Midinfrared Frequency Combs from Coherent Supercontinuum in Chalcogenide and Optical Parametric Oscillation', *Opt. Lett.*, **39**, 2056–2059 (2014).
54. K.F. Lee, C. Mohr, J. Jiang, P.G. Schunemann, K.L. Vodopyanov, M.E. Fermann, 'Midinfrared Frequency Comb from Self-stable Degenerate GaAs Optical Parametric Oscillator', *Opt. Express*, **23**, 26596–26603 (2015).
55. V. Muraviev, V.O. Smolski, Z.E. Loparo, K.L. Vodopyanov, 'Massively Parallel Sensing of Trace Molecules and Their Isotopologues with Broadband Subharmonic Mid-infrared Frequency Combs', *Nat. Photonics*, **12**, 209–214 (2018).
56. M.E. Fermann, I. Hartl, 'Ultrafast Fibre Lasers', *Nat. Photonics*, **7**, 868–874 (2013).

Encyclopedia of Analytical Chemistry, Online © 2006–2020 John Wiley & Sons, Ltd.

This article was published in the *Encyclopedia of Analytical Chemistry* in 2020 by John Wiley & Sons, Ltd.
DOI: 10.1002/9780470027318.a9321

57. I. Coddington, W.C. Swann, N.R. Newbury, 'Coherent Dual-comb Spectroscopy at High Signal-to-noise ratio', *Phys. Rev. A*, **82**, 043817 (2010).

58. F. Adler, P. Masłowski, A. Foltynowicz, K.C. Cossel, T.C. Briles, I. Hartl, J. Ye, 'Mid-infrared Fourier Transform Spectroscopy with a Broadband Frequency Comb', *Opt. Express*, **18**, 21861–21872 (2010).

59. Q. Ru, P. G. Schunemann, S. Vasilyev, S. B. Mirov, and K. L. Vodopyanov, 'A 2.35-μm pumped subharmonic OPO reaches the spectral width of two octaves in the mid-IR', in Conference on Lasers and Electro-Optics, OSA Technical Digest (Optical Society of America, 2019), SF1H.1.

Encyclopedia of Analytical Chemistry, Online © 2006–2020 John Wiley & Sons, Ltd.

This article was published in the *Encyclopedia of Analytical Chemistry* in 2020 by John Wiley & Sons, Ltd.
DOI: 10.1002/9780470027318.a9321